

# Reactive Molecular Dynamics Simulations of the Depolymerization of Polyethylene Using Graphene-Oxide-Supported Platinum Nanoparticles

Wengang Zhang,\* Francis W. Starr, Kathryn L. Beers, and Jack F. Douglas



Cite This: *J. Phys. Chem. A* 2022, 126, 3167–3173



Read Online

ACCESS |

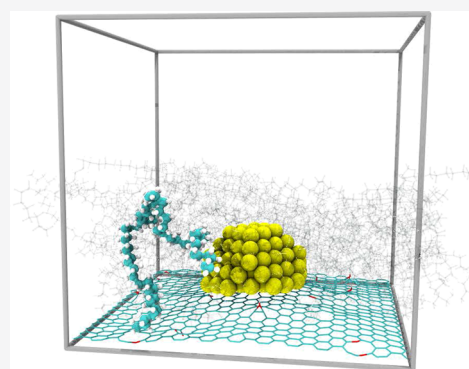


Metrics & More



Article Recommendations

**ABSTRACT:** While plastic materials offer many benefits to society, the slow degradation and difficulty in recycling plastics raise important environmental and sustainability concerns. Traditional recycling efforts often lead to materials with inferior properties and correspondingly lower value, making them uneconomical to recycle. Recent efforts have shown promising chemical pathways for converting plastic materials into a wide range of value-added products, feedstocks or monomers. This is commonly referred to as “chemical recycling”. Here, we use reactive molecular dynamics (MD) simulations to study the catalytic process of depolymerization of polyethylene (PE) using platinum (Pt) nanoparticles (NPs) in comparison to PE pyrolysis (thermal degradation). We apply a simple kinetic model to our MD results for the catalytic reaction rate as a function of temperature, from which we obtain the activation energy of the reaction, which shows that the Pt NPs reduce the barrier for depolymerization. We further evaluate the molecular mass distribution of the reaction products to gain insight into the influence of the Pt NPs on reaction selectivity. Our results demonstrate the potential for the reactive MD method to help the design of recycling approaches for polymer materials.



## 1. INTRODUCTION

The relative low cost and utility of plastic materials have led to a steady increase in the production and use of these materials in a wide range of applications, including packaging, home and personal products, diverse materials associated with health care and automotive materials, and increasingly in structural materials when plastics are compounded with carbon fibers and other materials that allow the composite materials to be tuned over a large range.<sup>1,2</sup> However, the low rate at which these materials degrade in the environment, combined with the limited economic incentive to recycle plastic materials, has led to accumulated polymer waste materials and an associated ecological problem when that waste is mismanaged; these factors have helped motivate organized efforts to address this growing societal concerns.<sup>3</sup> Geyer et al.<sup>4</sup> have recently reviewed the history of the production, the range of uses, and the ultimate fate of plastic materials.

Current strategies to address the plastic waste problem include recycling postconsumer plastics using either mechanical or chemical recycling.<sup>5</sup> While mechanical recycling, which often involves collecting, sorting, washing, and grinding of the post-consumer plastics, remains the most common method, the difficulty in separating various kinds of plastics and other foreign materials makes this approach less economically viable. In particular, mixed plastics have different melting and

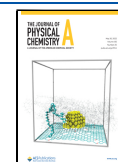
processing temperatures that lead to the thermal degradation of some plastics, resulting in poor product quality. Furthermore, the immiscibility of plastic blends can also decrease the mechanical strength of the polymers, though it can be mitigated by compatibilizers,<sup>6</sup> which can be designed to mix a specific pair of polymers.<sup>7</sup> On the other hand, chemical recycling aims to recover a significant fraction of the monomer material or value-added materials such as lubricants and waxes.<sup>5,7,14</sup> Typical chemical recycling processes include chemolysis (or depolymerization), pyrolysis, fluid catalytic cracking, and others.<sup>5,8–12</sup>

The present work considers the degree to which reactive molecular dynamics (MD) simulations can be used to help develop a better theoretical understanding of the depolymerization of waste plastics using a heterogeneous catalyst. This method transforms polymers into new “feedstock” materials from which new polymeric or other organic materials can be synthesized.<sup>12–16</sup> The goal of this chemical recycling is to

**Received:** February 17, 2022

**Revised:** April 25, 2022

**Published:** May 9, 2022



recover excess value from polymers that have passed through a wide range of uses. In particular, it is useful for plastics that are not suitable for mechanical pathways, such as multilaminates, textiles, previously mechanically recycled products, and environmentally degraded materials (for example, marine debris). It has been estimated that 90% of all chemical manufacturing processes make use of heterogeneous catalysis,<sup>17,18</sup> accounting for about 1/3 of the world's gross domestic product.<sup>19,20</sup> More specifically, the majority of industrial catalysts involve metal particles supported on nonreactive supporting materials with high-surface area.<sup>17,21</sup> Thus, this approach to the catalysis of materials at a large scale has a proven record in industrial utility and scalability.

Realizing the goal of chemically recycling otherwise challenging plastic materials and product formats requires an understanding of the catalytic conversion of polymers of diverse types using an economically viable process. Recently, significant progress in this direction was provided by Zhang et al.,<sup>13</sup> and the present work aims to model this type of heterogeneous catalysis process by reactive MD simulation.<sup>22–26</sup> These simulations offer a proof of the viability of reactive MD techniques to capture the depolymerization of polyethylene, and in doing so, understand the fundamental nature of the catalytic reaction processes in relation to the ultimate aim of offering design rules that could enhance the economic feasibility of this process.

We note at the outset that because of the limitations on accessible time scales in MD, our simulations are performed at temperatures ( $T$ ) above the range envisioned for reprocessing polymer waste to facilitate the reactions ( $\approx 300$  °C). We find that we can reproduce many of the qualitative aspects of the observed experimental trends in this type of catalysis by our reactive MD simulations, putting us in a good position to explore new approaches for further catalytic optimization, for example, the control of particle size, shape, “promotor” or “poisoning” additives, and so forth,<sup>27–35</sup> physical attributes of catalytically active NPs that are known to greatly influence reactivity. The fundamental origin of these variations in reactivity are currently poorly understood. Pan et al.<sup>36</sup> review attempts to understand the nature of the specific active sites that are presumably the origin of this variability of catalytic reactivity,<sup>27–34</sup> physical attributes of catalytically active NPs that are known to greatly influence reactivity. There are many physical aspects of heterogeneous catalysis using nanoparticles that require further significant research to optimize reactivity and the economic viability of this approach to the large-scale remediation of plastic waste materials to make polymers a renewable resource.

In the present work, we focus on a computational model for the depolymerization polyethylene (PE) using Pt NP supported by a graphene oxide substrate using reactive MD simulations. In doing so, we first contrast the depolymerization of PE with and without the Pt NP and demonstrate that the Pt NP is effective in catalyzing the depolymerization to form shorter chains. We next evaluate the average number of carbon atoms in each chain over the reaction time and establish a kinetic model from which we obtain the reaction rate for both PE with and without Pt NP. Because the reaction rates obey an Arrhenius relation, we can estimate the activation energy for depolymerization and show the reduction of the energy with the presence of the catalyst.

## 2. MODELING AND SIMULATION

Our results are based on the atomistic MD simulations of polyethylene and platinum nanoparticles supported by graphene-oxide. We use a reactive force field (ReaxFF),<sup>24</sup> in which the bond order is instantaneously dependent on the local atomic environment, and it is parametrized using the electronic structure methods. This force field can describe the energetics along the reaction path, allowing for the modeling of chemical reactions. In particular, we utilize ReaxFF for Pt/C/O/H<sup>23,26</sup> implemented in LAMMPS (Large-scale Atomic/Molecular Massively Parallel Simulator).<sup>37</sup> Our simulations are performed within the canonical ensemble (NVT) with  $T$  ranging from 1900 to 2400 K and density  $0.63\text{ g/cm}^3$  excluding Pt. Although these temperatures are significantly higher than those used in experiments, it is a common practice in computational studies to use higher temperatures to allow for reactions to occur in accessible computational time scale on the order of a few nanoseconds<sup>38–40</sup> and still provides insight into the catalytic reactions from a molecular level. Previous work<sup>41,42</sup> have shown that despite higher temperatures used in simulations, the estimated activation energy from simulations is similar to that from experiments and the results we shall show support this trend. In general, the ReaxFF method provides a reasonable trade-off between computationally more expensive quantum methods and less realistic coarse-grained methods. That said, it is still computationally prohibitive to simulate the chemical reaction for macromolecules at temperatures close to experimental conditions using ReaxFF. Moreover, our study more focuses on contrasting the relative performance of polyethylene with and without platinum nanoparticles rather than the absolute degree of depolymerization at various temperatures. Previously, this reactive force field has been successfully used to simulate the catalytic reaction of combustion,<sup>38,43</sup> fuel decomposition,<sup>39</sup> and pyrolysis,<sup>40,41</sup> with accuracy comparable to that from the electronic structure method. For more details on this force field, Senftle et al.<sup>44</sup> reviewed the recent development and application of ReaxFF.

In each simulation, we use 40 polyethylene molecules, each consisting of 30 monomers ( $\text{C}_{60}\text{H}_{122}$ ). For the simulations with the catalysts, the Pt NP is supported by graphene oxide. We also performed catalytic simulations of polyethylene without graphene oxide to contrast its (lack of) influence on the reaction. In simulations with the catalyst, we use Pt NP that are on the order of 2 nm. We performed at least three independent molecular configurations for each set of simulations to obtain better averages. We show a representative simulation snapshot for truncated octahedron NP with polyethylene in Figure 1.

## 3. RESULTS AND DISCUSSION

We first demonstrate the ability of the reactive MD approach to reproduce the catalytic effect of a Pt NP on the decomposition of polyethylene. Figure 2 shows the percentage of polyethylene that no longer retains its original chain length as a function of time at  $T = 2200\text{ K}$ . We observe that in the presence of a Pt NP, PE decomposes faster to shorter alkanes than simple thermal degradation of pure polyethylene (black curve), indicated by the higher conversion percentage of the catalytic system (red curve). Polyethylene with a Pt NP, but without graphene oxide (green curve), shows a similar conversion rate compared to the case of PE with the Pt NP alone. This result is in contrast to the catalytic fuel

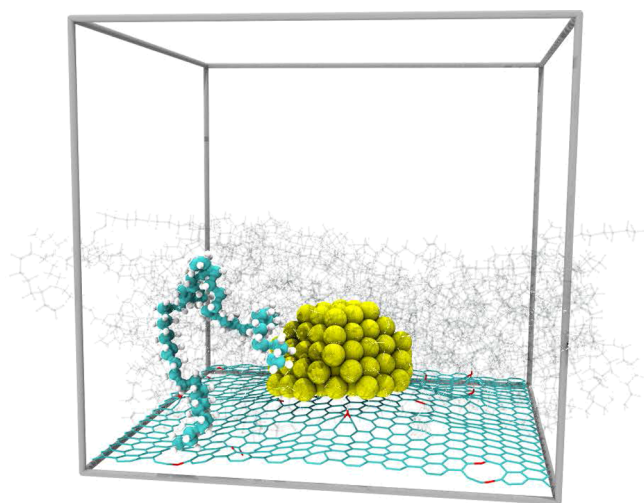


**Figure 1.** A simulation snapshot of polyethylene molecules with a platinum nanoparticle supported on graphene oxide. Only two representative PE chains are rendered as the ball-and-stick model, and the rest are rendered as translucent wireframe molecules for visual clarity.

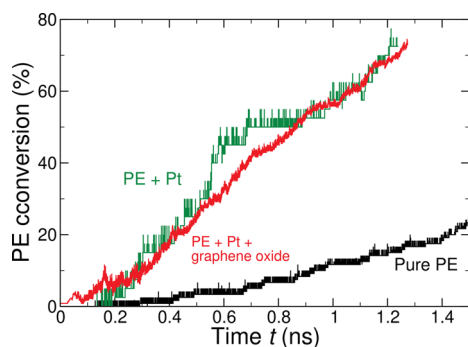


**Figure 2.** Percentage of the original polyethylene chains converted to shorter chains at  $T = 2200$  K. Each curve data are averaged over at least two molecular trajectories.

decomposition using graphene-supported Pt NPs,<sup>39</sup> where graphene oxide enhances the reaction rate. The difference might be due to the higher molecular mass and density of hydrocarbons used in our simulations. Specifically, both the longer polymer chains and higher density significantly lower molecular mobility, resulting in the slower turnover rate for the polymers near the Pt surface. Additionally, considering one of the main purposes of the supporting substrate is to decrease

the change of NP aggregation, and because we eliminate the possibility of NP aggregation by using single NP in our simulations, it is reasonable to see that simulations either with or without graphene oxide shows the same PE conversion percentage. We also examine the conversion rate for other NP shapes, such as square pyramid and cube, and we do not find statistically significant differences between them, presumably a result of the high temperature used in our simulations.

Having demonstrated the effectiveness of Pt NPs to facilitate the decomposition of polyethylene, we next examine the time evolution of the average molecule size of the decomposed PE at various  $T$  in Figure 3. Specifically, we evaluate the ensemble-averaged number of carbon atoms (average carbon number) in each polyethylene molecule as a function of time, as shown in Figure 3. Consistent with the PE conversion percentage shown in Figure 2, the average carbon number decreases significantly over time in the presence of Pt NP (Figure 3a). As for the temperature dependence of the average carbon number shown in Figure 3b, we see that the average carbon number decreases more significantly over time as  $T$  increases. Although it would be ideal if we could simulate the catalytic reaction of polyethylene at a lower temperature to avoid the complicating influence of pyrolysis, we are constrained by the fact that below  $T = 1800$  K, polyethylene does not depolymerize with or without a catalyst in the accessible timescale. Nevertheless, our results show the improved depolymerization of polyethylene with a catalyst. Having shown the time dependence of the average carbon number, we next utilize this information to establish a kinetic model to describe the rate constant of the depolymerization process.

**3.1. Reaction Kinetic Model.** The catalytic reaction of the depolymerization of PE is assumed to be a zero-order reaction because of the attractive interaction between PE and Pt NP, and the surface of Pt NP is typically saturated with polymer chains. The reaction rate  $\gamma_{\text{depoly}}$  is approximately estimated from the change of the number of polymer chains with time  $t$ ,

$$\frac{dN(t)}{dt} = \gamma_{\text{depoly}} \quad (1)$$

where  $N$  is the number of molecules, and  $\gamma_{\text{depoly}}$  is the rate of depolymerization (or the rate of C–C bond breakage).  $\gamma_{\text{depoly}}$  is a constant, and it is only dependent on the fraction of Pt in the system. By the integration of eq 2 over time, we obtain  $N(t) = N_0 + \gamma_{\text{depoly}} t$ , where  $N_0$  is the initial number of polymer chains. The average number of carbons per chain  $M_c$  as a function of time  $t$  is expressed as

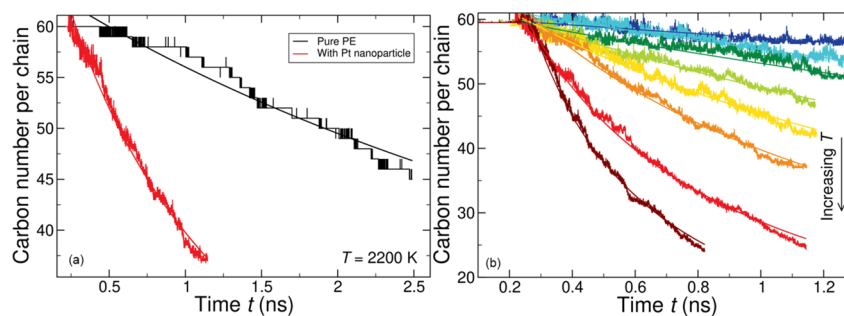


**Figure 3.** (a) Comparison between the decomposition of pure PE and depolymerization using Pt NP at  $T = 2200$  K. (b) Time dependence of the average carbon numbers per chain for various temperatures  $T$  ranging from 1900 to 2400 K. The presence of Pt NPs significantly facilitates the depolymerization of PE. The smooth curves are the fits using eq 2.

$$\langle M_c(t) \rangle = \frac{N_0 M_c(0)}{N_0 + \gamma_{\text{depoly}} t} \quad (2)$$

We use eq 2 to fit the time evolution of the average carbon number of PE chains, as shown in Figure 3b, from which we obtain the rate of depolymerization  $\gamma_{\text{depoly}}$  as a fitting parameter. Because the mass of Pt nanoparticles remains the same for all simulations considered, the rate of depolymerization  $\gamma_{\text{depoly}}$  is proportional to the reaction rate constant  $k$  (or  $\gamma_{\text{depoly}} = m_{\text{Pt}} k$ ). Using this method, we obtain rate constants  $k$  for all temperatures and systems considered and plot this quantity against the inverse temperature  $1/T$  in Figure 4.

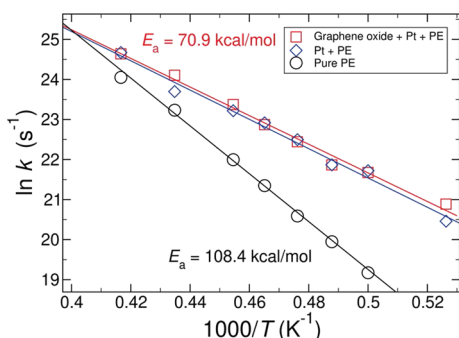


**Figure 4.** Rate constant  $k$  as a function of inverse temperature ( $1000/T$ ). The “crossover temperature” or “isokinetic temperature” for the two Arrhenius curves is near 2500 K, where  $\ln A = 40.42$  with Pt and  $\ln A = 49.03$  for pure PE.

The Arrhenius plot in Figure 4 shows that the presence of Pt NP facilitates the catalytic reactions lowering the activation energy. To quantify the activation energy, we fit the rate constant in Figure 4 using the Arrhenius equation,

$$\ln k = \ln A - \frac{E_a}{RT} \quad (3)$$

where  $A$  is the prefactor,  $E_a$  is the activation energy, and  $R$  is the gas constant. We find that the activation energies are approximately 108.4 and 70.9 kcal/mol for the pure PE and PE with Pt NPs, respectively. Evidently, the Pt NP lowers the activation energy for breaking down PE. In comparison, the effective activation energy of PE pyrolysis in experiments is estimated to be 89 kcal/mol for low-density polyethylene (LDPE), while the catalytic activation energy is approximately 80 kcal/mol,<sup>45</sup> although zeolite is used as the catalyst. Thus, our simulation estimates are consistent with those of experiments. Moreover, we do not observe a significant degree of adsorption of hydrogen atoms onto the catalyst surface that would result in a reduction in the reactivity. This is consistent with the reaction kinetic model, which assumes that polyethylene is always in contact with the catalyst; the reaction rate (Figure 3b) is well-described using this model. Experiments also find that the degradation of the catalyst is minimal.<sup>13</sup>

**3.2. Reaction Product Analysis.** Having quantified the activation energy for the reaction, we next examine the composition and mass distribution of reaction products. We group hydrocarbon products into several intervals based on the number of carbon atoms in the molecule for all cases studied and evaluate the ensemble average for the mass fraction of molecules in each carbon number interval shown in Figure 5. This carbon number distributions are evaluated at the same simulation time (0.8 ns) across all cases. It should be noted that the mass fraction here only accounts for the fraction of carbon atoms in each interval among all carbon atoms in the simulation. In other words, hydrogen, platinum, and oxygen atoms are not considered in the mass fraction.

Figure 5a shows the carbon mass fraction for each group at various temperatures in the case of pure PE. At the lowest  $T$  considered ( $T = 2000$  K), nearly all PE chains fall in the  $C_{51}$ – $C_{60}$  category, meaning almost no pyrolysis reactions occurred. We also see that, within each carbon group, the mass fraction increases with increasing temperature, except for the highest carbon group  $C_{51}$ – $C_{60}$ . This is expected because the degree of pyrolysis increases with increasing  $T$ . Furthermore, because

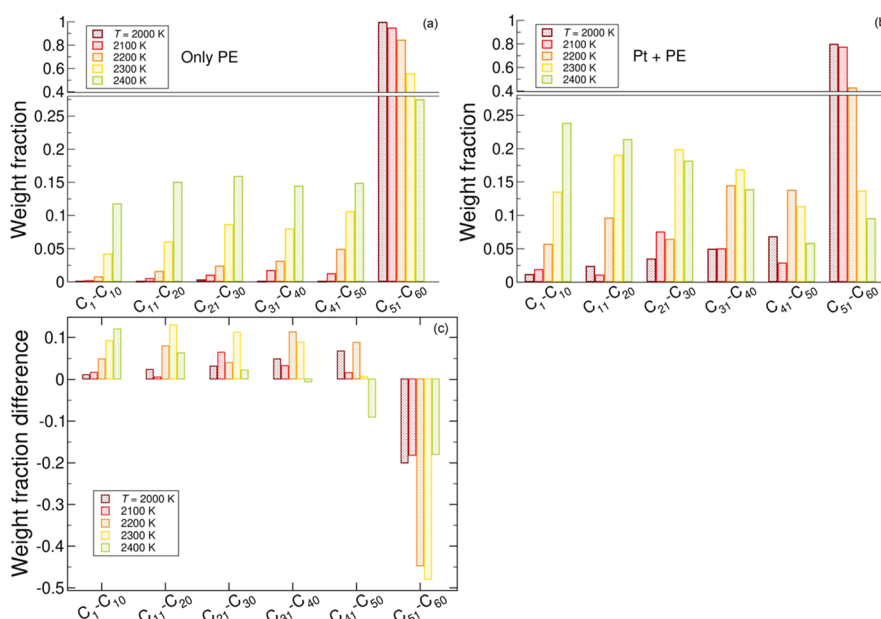


**Figure 5.** Distribution of the mass fraction of reaction products for pure PE (a) and Pt with PE (b). (c) The difference between the mass fraction of Pt + PE and only PE.

pure PE only has a somewhat mild degree of pyrolysis overall, the mass fraction in the  $C_{51}$ – $C_{60}$  category has the highest weight fraction (the initial carbon number for each chain is  $C_{60}$  before the reaction). With the addition of Pt NPs (Figure 5b), the depolymerization of PE increases significantly with the increasing carbon mass fractions in the lower range category compared to the case shown in Figure 5a.

At higher  $T$ , we find that the mass fraction is generally higher at lower carbon number groups (Figure 5b) because the catalytic behavior of Pt NPs and pyrolysis in tandem further enhance depolymerization, especially the pyrolysis, which has the tendency to breakdown PE into smaller and nonuniformly distributed hydrocarbons.<sup>13,40</sup> In contrast, at lower temperatures, the mass fraction distributions over all carbon intervals have a peak, indicating the Pt NP is selective on the product molecular mass and that selectivity depends on  $T$  (Figure 5b). Another way to quantify these effects is through taking the difference between the mass fraction of PE with Pt and PE only in Figure 5a,b, and the result is shown in Figure 5c. The presence of Pt NPs selectively produces a certain range of hydrocarbons depending on  $T$ . For example, at  $T = 2200$  K (orange bar), the mass fraction difference peaks in the  $C_{31}$ – $C_{40}$  range.

To further examine the potential effects of the supporting substrate graphene oxide, we next consider the volatile content of the reaction. Specifically, we study the fraction of hydrogen molecules for various  $T$  in all cases studied in Figure 6. The

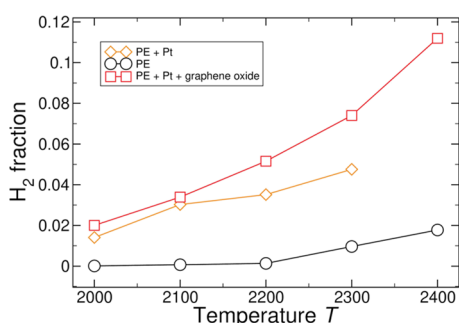


**Figure 6.** Hydrogen molecules in the reaction products at various  $T$ . The  $H_2$  fraction is evaluated from the ratio of  $H_2$  molecules to all hydrogen atoms in the system.

fraction of hydrogen molecules is evaluated as the fraction of hydrogen atoms in hydrogen molecules among all hydrogen atoms in the simulation. We find that as  $T$  increases, more  $H_2$  gas is generated, as expected because the Pt NP attracts and removes hydrogen from the hydrocarbons during the catalytic dehydrogenation process, and the adsorbed hydrogen atoms “roam” on the Pt surface, forming hydrogen molecules, and subsequently desorb from the Pt surface.<sup>39</sup> Furthermore, we find that simulations with graphene oxide yield more  $H_2$  than those without graphene oxide. It is thought that the migration of hydrogen atoms to the graphene oxide surface facilitates the desorption of  $H_2$ .<sup>39,46,47</sup> Indeed, the activation energy barrier from density function theory calculations<sup>46,47</sup> shows that the energy barrier is estimated to be greater than 60 kcal/mol, smaller than the activation energy for the depolymerization estimated in this work. An experimental study of depolymerization of PE by Pt NPs at lower  $T$  (280 °C) by Zhang et al.<sup>13</sup> indicated that alkylaromatic compounds are formed in the products. While the aromatization of  $n$ -alkane by the Pt NPs

results in  $H_2$  gas, these reactions are favorable under the mild conditions (“lower” temperature and ambient pressure), while we only observe trace amounts of aromatic compounds in the reactive depolymerization of PE in the presence of Pt NPs at relatively high temperature.

## 4. CONCLUSIONS

One of the emerging methods for mitigating the plastic waste problems is to use catalytic processes to breakdown the long polymer chains of plastic molecules, such as PE, into smaller, more valuable oligomers and small molecules. In this work, we use reactive MD simulations to model the catalytic chemical conversion of PE using Pt NPs. Specifically, we combine PE molecules with the catalyst, Pt NP supported by graphene oxide, and confirm that the simulations can capture a catalytic effect that facilitates the hydrogenolysis reaction. We also evaluate the activation energy of both the catalytic reaction and PE pyrolysis and find that the activation energy is indeed lower for the catalytic reaction as expected. Furthermore, we show the selectivity in the molecular mass distribution of the catalytic reaction products. While using Pt NP to catalyze the hydrogenolysis of PE has been shown experimentally, to our knowledge, this work represents the first use of reactive atomistic MD simulations to demonstrate this phenomenon for PE. This work paves the road for further understanding the dynamics of Pt NP under the catalytic conditions and the detailed reaction mechanism. This computational model is well-suited for large-scale exploration in the design space of various sizes and spacing of NPs to find the optimal configuration for the desired composition of the reaction products. We anticipate that this computational methodology will be a useful tool in the design and characterization of new catalysts when combined with experiments.

## AUTHOR INFORMATION

### Corresponding Author

**Wengang Zhang** – Materials Science and Engineering Division, Material Measurement Laboratory, National Institute of Standards and Technology, Gaithersburg, Maryland 20899, United States; Department of Physics, Wesleyan University, Middletown, Connecticut 06459, United States; [orcid.org/0000-0001-9653-6966](https://orcid.org/0000-0001-9653-6966); Email: [wzhang01@wesleyan.edu](mailto:wzhang01@wesleyan.edu)

### Authors

**Francis W. Starr** – Department of Physics, Wesleyan University, Middletown, Connecticut 06459, United States; [orcid.org/0000-0002-2895-6595](https://orcid.org/0000-0002-2895-6595)

**Kathryn L. Beers** – Materials Science and Engineering Division, Material Measurement Laboratory, National Institute of Standards and Technology, Gaithersburg, Maryland 20899, United States

**Jack F. Douglas** – Materials Science and Engineering Division, Material Measurement Laboratory, National Institute of Standards and Technology, Gaithersburg, Maryland 20899, United States; [orcid.org/0000-0001-7290-2300](https://orcid.org/0000-0001-7290-2300)

Complete contact information is available at:  
<https://pubs.acs.org/10.1021/acs.jpca.2c01167>

### Notes

The authors declare no competing financial interest.

## ACKNOWLEDGMENTS

Computer time was provided by the National Institute of Standards and Technology (NIST) and Wesleyan University. This work was supported, in part, by NIST Award No. 70NANB19H137.

## REFERENCES

- (1) Morgan, P. *Carbon Fibers and Their Composites*; CRC Press, 2005.
- (2) Forintos, N.; Czigany, T. Multifunctional Application of Carbon Fiber Reinforced Polymer Composites: Electrical Properties of the Reinforcing Carbon Fibers – A Short Review. *Compos. Part B Eng.* **2019**, *162*, 331–343.
- (3) Jambeck, J. R.; Geyer, R.; Wilcox, C.; Siegler, T. R.; Perryman, M.; Andrady, A.; Narayan, R.; Law, K. L. Plastic Waste Inputs from Land into the Ocean. *Science* **2015**, *347*, 768–771.
- (4) Geyer, R.; Jambeck, J. R.; Law, K. L. Production, Use, and Fate of All Plastics Ever Made. *Sci. Adv.* **2017**, *3*, No. e1700782.
- (5) Ragaert, K.; Delva, L.; Van Geem, K. Mechanical and Chemical Recycling of Solid Plastic Waste. *Waste Manage.* **2017**, *69*, 24–58.
- (6) Koning, C.; Van Duin, M.; Pagnoulle, C.; Jerome, R. Strategies for Compatibilization of Polymer Blends. *Prog. Polym. Sci.* **1998**, *23*, 707–757.
- (7) Zhao, X.; Korey, M.; Li, K.; Copenhaver, K.; Tekinalp, H.; Celik, S.; Kalaitzidou, K.; Ruan, R.; Ragauskas, A. J.; Ozcan, S. Plastic Waste Upcycling toward a Circular Economy. *Chem. Eng. J.* **2022**, *428*, No. 131928.
- (8) Westhues, S.; Idel, J.; Klankermayer, J. Molecular Catalyst Systems as Key Enablers for Tailored Polyesters and Polycarbonate Recycling Concepts. *Sci. Adv.* **2018**, *4*, No. eaat9669.
- (9) Nakaji, Y.; Tamura, M.; Miyaoka, S.; Kumagai, S.; Tanji, M.; Nakagawa, Y.; Yoshioka, T.; Tomishige, K. Low-Temperature Catalytic Upgrading of Waste Polyolefinic Plastics into Liquid Fuels and Waxes. *Appl. Catal. B Environ.* **2021**, *285*, No. 119805.
- (10) Jia, X.; Qin, C.; Friedberger, T.; Guan, Z.; Huang, Z. Efficient and Selective Degradation of Polyethylenes into Liquid Fuels and Waxes under Mild Conditions. *Sci. Adv.* **2016**, *2*, No. e1501591.
- (11) Bäckström, E.; Odelius, K.; Hakkarainen, M. Designed from Recycled: Turning Polyethylene Waste to Covalently Attached Polylactide Plasticizers. *ACS Sustainable Chem. Eng.* **2019**, *7*, 11004–11013.
- (12) Tennakoon, A.; Wu, X.; Paterson, A. L.; Patnaik, S.; Pei, Y.; LaPointe, A. M.; Ammal, S. C.; Hackler, R. A.; Heyden, A.; Slowing, I. I.; Coates, G. W.; Delferro, M.; Peters, B.; Huang, W.; Sadow, A. D.; Perras, F. A. Catalytic Upcycling of High-Density Polyethylene via a Processive Mechanism. *Nat. Catal.* **2020**, *3*, 893–901.
- (13) Zhang, F.; Zeng, M.; Yappert, R. D.; Sun, J.; Lee, Y. H.; LaPointe, A. M.; Peters, B.; Abu-Omar, M. M.; Scott, S. L. Polyethylene Upcycling to Long-Chain Alkylaromatics by Tandem Hydrogenolysis/Aromatization. *Science* **2020**, *370*, 437–441.
- (14) Celik, G.; Kennedy, R. M.; Hackler, R. A.; Ferrandon, M.; Tennakoon, A.; Patnaik, S.; Lapointe, A. M.; Ammal, S. C.; Heyden, A.; Perras, F. A.; Pruski, M.; Scott, S. L.; Poeppelmeier, K. R.; Sadow, A. D.; Delferro, M. Upcycling Single-Use Polyethylene into High-Quality Liquid Products. *ACS Cent. Sci.* **2019**, *5*, 1795–1803.
- (15) Rorrer, J. E.; Beckham, G. T.; Román-Leshkov, Y. Conversion of Polyolefin Waste to Liquid Alkanes with Ru-Based Catalysts under Mild Conditions. *JACS Au* **2021**, *1*, 8–12.
- (16) Ellis, L. D.; Orski, S. V.; Kenlaw, G. A.; Norman, A. G.; Beers, K. L.; Román-Leshkov, Y.; Beckham, G. T. Tandem Heterogeneous Catalysis for Polyethylene Depolymerization via an Olefin-Intermediate Process. *ACS Sustainable Chem. Eng.* **2021**, *9*, 623–628.
- (17) Jimenez-Izal, E.; Alexandrova, A. N. Computational Design of Clusters for Catalysis. *Annu. Rev. Phys. Chem.* **2018**, *69*, 377–400.
- (18) Ertl, G.; Knözinger, H.; Weitkamp, J. *Handbook of Heterogeneous Catalysis*; Ertl, G., Knözinger, H., Schüth, F., Weitkamp, J., Eds.; Wiley-VCH Verlag GmbH & Co. KGaA: Weinheim, Germany, 2008; 1–5.
- (19) Zaera, F. Outstanding Mechanistic Questions in Heterogeneous Catalysis. *J. Phys. Chem. B* **2002**, *106*, 4043–4052.
- (20) Martino, G. Catalysis for Oil Refining and Petrochemistry, Recent Developments and Future Trends. In *Studies in Surface Science and Catalysis*; 2000; *130*, 83–103.
- (21) Bell, A. T. The Impact of Nanoscience on Heterogeneous Catalysis. *Science* **2003**, *299*, 1688–1691.
- (22) Mueller, J. E.; van Duin, A. C. T.; Goddard, W. A., III; Pennsylv, V. Hydrocarbon Chemistry Catalyzed by Nickel. *J. Phys. Chem. C* **2010**, *114*, 4939–4949.
- (23) Shin, Y. K.; Gai, L.; Raman, S.; van Duin, A. C. T. Development of a ReaxFF Reactive Force Field for the Pt–Ni Alloy Catalyst. *J. Phys. Chem. A* **2016**, *120*, 8044–8055.
- (24) Chenoweth, K.; van Duin, A. C. T.; Goddard, W. A. ReaxFF Reactive Force Field for Molecular Dynamics Simulations of Hydrocarbon Oxidation. *J. Phys. Chem. A* **2008**, *112*, 1040–1053.
- (25) Chenoweth, K.; van Duin, A. C. T.; Persson, P.; Cheng, M. J.; Ongaard, J.; Goddard, W. A. Development and Application of a ReaxFF Reactive Force Field for Oxidative Dehydrogenation on Vanadium Oxide Catalysts. *J. Phys. Chem. C* **2008**, *112*, 14645–14654.
- (26) Gai, L.; Shin, Y. K.; Raju, M.; van Duin, A. C. T.; Raman, S. Atomistic Adsorption of Oxygen and Hydrogen on Platinum Catalysts by Hybrid Grand Canonical Monte Carlo/Reactive Molecular Dynamics. *J. Phys. Chem. C* **2016**, *120*, 9780–9793.
- (27) Ahmadi, T. S.; Wang, Z. L.; Green, T. C.; Henglein, A.; El-Sayed, M. A. Shape-Controlled Synthesis of Colloidal Platinum Nanoparticles. *Science* **1996**, *272*, 1924–1925.
- (28) Narayanan, R.; El-Sayed, M. A. Catalysis with Transition Metal Nanoparticles in Colloidal Solution: Nanoparticle Shape Dependence and Stability. *J. Phys. Chem. B* **2005**, *109*, 12663–12676.
- (29) Narayanan, R.; El-Sayed, M. A. Shape-Dependent Catalytic Activity of Platinum Nanoparticles in Colloidal Solution. *Nano Lett.* **2004**, *4*, 1343–1348.
- (30) Bartholomew, C. H.; Agrawal, P. K.; Katzer, J. R. Sulfur Poisoning of Metals. *Adv. Catal.* **1982**, *31*, 135–242.
- (31) Zhou, X.; Xu, W.; Liu, G.; Panda, D.; Chen, P. Size-Dependent Catalytic Activity and Dynamics of Gold Nanoparticles at the Single-Molecule Level. *J. Am. Chem. Soc.* **2010**, *132*, 138–146.
- (32) Lee, I.; Delbecq, F.; Morales, R.; Albitzer, M. A.; Zaera, F. Tuning Selectivity in Catalysis by Controlling Particle Shape. *Nat. Mater.* **2009**, *8*, 132–138.
- (33) Yang, J.; Lee, J. Y.; Too, H. P. Size Effect in Thiol and Amine Binding to Small Pt Nanoparticles. *Anal. Chim. Acta* **2006**, *571*, 206–210.
- (34) Zhang, J.; Xu, H.; Li, W. Kinetic Study of NH<sub>3</sub> Decomposition over Ni Nanoparticles: The Role of La Promoter, Structure Sensitivity and Compensation Effect. *Appl. Catal. A Gen.* **2005**, *296*, 257–267.
- (35) Li, Z.; Ji, S.; Liu, Y.; Cao, X.; Tian, S.; Chen, Y.; Niu, Z.; Li, Y. Well-Defined Materials for Heterogeneous Catalysis: From Nanoparticles to Isolated Single-Atom Sites. *Chem. Rev.* **2020**, *120*, 623–682.
- (36) Pan, Y.; Shen, X.; Yao, L.; Bentalib, A.; Peng, Z. Active Sites in Heterogeneous Catalytic Reaction on Metal and Metal Oxide: Theory and Practice. *Catalysts* **2018**, *8*, 478.
- (37) Plimpton, S. Fast Parallel Algorithms for Short-Range Molecular Dynamics. *J. Comput. Phys.* **1995**, *117*, 1–19.
- (38) Feng, M.; Jiang, X. Z.; Luo, K. H. A Reactive Molecular Dynamics Simulation Study of Methane Oxidation Assisted by Platinum/Graphene-Based Catalysts. *Proc. Combust. Inst.* **2019**, *37*, 5473–5480.
- (39) Sim, H. S.; Yetter, R. A.; Hong, S.; van Duin, A. C. T.; Dabbs, D. M.; Aksay, I. A. Enhanced Fuel Decomposition in the Presence of Colloidal Functionalized Graphene Sheet-Supported Platinum Nanoparticles. *ACS Appl. Energy Mater.* **2020**, *3*, 7637–7648.
- (40) Liu, X.; Li, X.; Liu, J.; Wang, Z.; Kong, B.; Gong, X.; Yang, X.; Lin, W.; Guo, L. Study of High Density Polyethylene (HDPE) Pyrolysis with Reactive Molecular Dynamics. *Polym. Degrad. Stab.* **2014**, *104*, 62–70.

- (41) Chenoweth, K.; van Duin, A. C. T.; Dasgupta, S.; Goddard III, W. A. Initiation Mechanisms and Kinetics of Pyrolysis and Combustion of JP-10 Hydrocarbon Jet Fuel. *J. Phys. Chem. A* **2009**, *113*, 1740–1746.
- (42) Mao, Q.; Van Duin, A. C. T.; Luo, K. H. Investigation of Methane Oxidation by Palladium-Based Catalyst via ReaxFF Molecular Dynamics Simulation. *Proc. Combust. Inst.* **2017**, *36*, 4339–4346.
- (43) Weismiller, M. R.; van Duin, A. C. T.; Lee, J.; Yetter, R. A. ReaxFF Reactive Force Field Development and Applications for Molecular Dynamics Simulations of Ammonia Borane Dehydrogenation and Combustion. *J. Phys. Chem. A* **2010**, *114*, 5485–5492.
- (44) Senftle, T. P.; Hong, S.; Islam, M. M.; Kylasa, S. B.; Zheng, Y.; Shin, Y. K.; Junkermeier, C.; Engel-Herbert, R.; Janik, M. J.; Aktulga, H. M.; Verstraelen, T.; Grama, A.; Van Duin, A. C. T. The ReaxFF Reactive Force-Field: Development, Applications and Future Directions. *npj Comput. Mater.* **2016**, *2*, 1511.
- (45) Miskolczi, N.; Bartha, L.; Deák, G. Y.; Jóver, B.; Kalló, D. Kinetic Model of the Chemical Recycling of Waste Polyethylene into Fuels. *Process Saf. Environ. Prot.* **2004**, *82*, 223–229.
- (46) Psfogiannakis, G. M.; Froudakis, G. E. DFT Study of Hydrogen Storage by Spillover on Graphite with Oxygen Surface Groups. *J. Am. Chem. Soc.* **2009**, *131*, 15133–15135.
- (47) Psfogiannakis, G. M.; Froudakis, G. E. DFT Study of the Hydrogen Spillover Mechanism on Pt-Doped Graphite. *J. Phys. Chem. C* **2009**, *113*, 14908–14915.

## Recommended by ACS

### Rational Design of Chemical Catalysis for Plastic Recycling

Mingyu Chu, Jinxing Chen, *et al.*

APRIL 05, 2022  
ACS CATALYSIS

READ 

### Tandem Catalysts for Polyethylene Upcycling: A Simple Kinetic Model

Damien Guironnet and Baron Peters

APRIL 20, 2020  
THE JOURNAL OF PHYSICAL CHEMISTRY A

READ 

### Upcycling Single-Use Polyethylene into High-Quality Liquid Products

Gokhan Celik, Massimiliano Delferro, *et al.*

OCTOBER 23, 2019  
ACS CENTRAL SCIENCE

READ 

### Extraction of Biolubricant via Chemical Recycling of Thermosetting Polymers

Xiao Kuang, H. Jerry Qi, *et al.*

MARCH 05, 2019  
ACS SUSTAINABLE CHEMISTRY & ENGINEERING

READ 

Get More Suggestions >